Analysis of (p,p), (p,n), and (n,n) scattering on the even tin isotopes using the Lane coupled equations

C. Wong and S. M. Grimes*
University of California, Lawrence Livermore National Laboratory, Livermore, California 94550

R. W. Finlay
Ohio University, Athens, Ohio 45701
(Received 27 December 1983)

(p,p), (p,n), and (n,n) scattering on ^{116,118,120,122,124}Sn have been analyzed employing the Lane coupled equations. The (p,n) measurements were made at $E_p = 24.5$ MeV, the appropriate energy at which to complement existing (p,p) measurements at 24.5 MeV and (n,n) measurements at 11 MeV. A search routine on the Lane coupled equations code yielded the complex isovector and isoscalar strengths from the simultaneous fitting of (p,p) and (p,n) data. These strengths have provided excellent fits to the (n,n) data on all five tin isotopes. The near constancy of the real and imaginary isovector strengths with A implies that the effects of channel coupling to the first 2^+ and 3^- states are either small or fairly uniform over the isotopic sequence. The implications of the Lane coupled equations with regard to the Coulomb correction on the imaginary optical potential are discussed.

INTRODUCTION

The diagonal and nondiagonal matrix elements of the Lane potential,[1]

$$U = U_0 + \frac{U_1}{A}\vec{t}\cdot\vec{T}\,, \tag{1}$$

connect (p,p) and (n,n) elastic and (p,n) quasielastic scattering as follows:

$$\begin{aligned} U_{pp} &= U_0 + \frac{U_1}{4A}(N-Z)\,, \\ U_{nn} &= U_0 - \frac{U_1}{4A}(N-Z)\,, \\ U_{pn} &= \frac{U_1}{2A}\sqrt{N-Z}\,. \end{aligned} \tag{2}$$

The Lane potential is clearly charge independent; the absence of the Coulomb interaction would suggest that the (p,p), (n,n), and (p,n) potentials should be compared at the same bombarding energy. This is valid if the proton bombarding energy is much greater than the Coulomb displacement energy (CDE), the negative of which is the Q value for the isobaric analog transition. For lower bombarding energies, Lane[1] provided in the Appendix to his paper a formal basis for the treatment of Coulomb effects. In effect, the resulting Lane coupled equations[1] imply that Eq. (2) is still valid provided that U_{nn} describes neutron elastic scattering at a bombarding energy which is lower than the incident proton energy by the CDE. Specifically, the Lane coupled equations imply that at bombarding energies differing by the CDE, the isoscalar (U_0) and isovector (U_1) strengths are identical for protons and neutrons. As shown in the Appendix to this paper, this is possible in the DWBA approach if U_0 and U_1 (both complex) are linearly dependent on bombarding energy and if U_{pp} is parametrized with the full Coulomb correction[2,3] for both real and imaginary parts.

The usual Coulomb correction[2] as applied to the parametrization of the real potential assumes that, aside from the change of sign of the isovector term, the proton and neutron isoscalar and isovector real strengths are identical when evaluated at the same average kinetic energy inside the nucleus. For protons, this occurs when the proton incident energy is reduced by the average Coulomb potential energy given by $1.38Z/A^{1/3}$ (MeV) for $r_0 = 1.25$ fm and is referred to as the full Coulomb correction. Since $1.38Z/A^{1/3} \cong$ CDE, the stipulations of the Lane coupled equations are thus tantamount to making the full Coulomb correction for both real and imaginary potentials. The full Coulomb correction for the real potential is well understood[2] and widely used in parametrizing the real potential.[2,3] The imaginary Coulomb correction[4] as a function of energy and mass number is less well established. Therefore a test of the Lane coupled equations can be viewed as a check on the applicability of a full Coulomb correction to the imaginary optical potential.

Carlson *et al.*[5] utilized the Becchetti-Greenlees[3] (BG) best-fit proton parametrization in their global analysis of (p,p), (p,n), and (n,n) scattering. As a result, their DWBA analysis incorporated the full Coulomb correction in the real potential and no Coulomb correction in the imaginary potential. The best-fit isovector interaction parameters determined from the quasielastic data were used in conjunction with the BG best-fit proton optical model parameters to generate the neutron optical potential by reversing the sign of the isovector terms. Predictions of neutron elastic scattering were then obtained and compared with measurements for five nuclei at neutron bombarding energies which were lower by approximately the CDE. Good agreement was observed for Fe, Ni, Zn, In, and Sn(n,n). On the other hand, a similar analysis by Schery *et al.*,[6] on the heavy nuclei between ^{197}Au and ^{232}Th, did not yield

predictions which agreed with measured neutron elastic scattering data.

Using the DWBA, Patterson *et al.*[7] obtained simultaneous fits to global (p,p) elastic and (p,n) quasielastic data at 25, 35, and 45 MeV, the (p,p) data being generated via the BG (Ref. 3) global Coulomb-corrected proton potential. The energy dependent isovector and isoscalar strengths so obtained were reasonably successful in reproducing (n,n) scattering on Al, Fe, Sn, and Bi at 7, 14, and 24 MeV. It should be noted, however, that Patterson *et al.*[7] employed 0.6 times the full Coulomb potential energy correction or $0.84Z/A^{1/3}$ MeV in the parametrization of both the real and imaginary proton potentials.

The work of Carlson *et al.* and Patterson *et al.* would indicate that the simultaneous fitting of global (n,n), (p,p), and (p,n) data requires less than the full Coulomb correction in the imaginary proton potentials. To check the appropriateness of the use of the full Coulomb correction for the imaginary potential, the Lane coupled equations were applied to (p,p), (n,n), and (p,n) scattering on the even tin isotopes. The (p,n) measurements were obtained at $E_p=24.5$ MeV, the appropriate energy to complement (p,p) scattering measurements[8] at 24.5 MeV and (n,n) measurements[9] at 11 MeV. Such an analysis on a series of isotopes at bombarding energies specified by the Lane coupled equations provides a less ambiguous test of the applicability of the coupled equations (and appropriateness of a full imaginary Coulomb correction) since any lack of detailed agreement cannot then be attributed to the use of global potentials and/or comparisons with measurements at not precisely the appropriate bombarding energies.

EXPERIMENTAL METHOD

The 24.5 MeV protons were accelerated by the Lawrence Livermore National Laboratory Cyclograaff.[10] A 15 MeV $^1H^-$ beam was extracted from the 80-cm fixed-energy cyclotron and was swept to reduce the burst rate from 25 to 2.5 MHz. The beam was then injected into an EN Tandem Van de Graaff for acceleration to the final energy. The average beam current on target was typically 60 nA; the burst width was typically 2.5 ns FWHM, corresponding to an energy spread of 0.23 MeV for 11 MeV neutrons.

The tin targets (isotopic enrichments $\geq 93\%$) were self-supporting metal foils of around 4 mg/cm^2 thickness. Sixteen collimated 10.75 m flight paths (see Fig. 1 of Ref. 11), which span the angular region from 3.5° to 159°, were employed for simultaneous data acquisition. To prevent overlap in the time-of-flight spectrum of low energy neutrons with high energy neutrons from a subsequent burst, a neutron detector bias of 5.4 MeV was employed. Pulse shape discrimination was employed on the sixteen 11.4 cm diameter by 5.1 cm thick NE213 scintillators to reduce the gamma ray background. The stop pulses into the time-to-amplitude converter were generated by a channel electron multiplier[12] which detected secondary electrons emitted from a thin (20 μg/cm^2) carbon foil located about 90 cm in front of the target. For a discussion of the neutron detector efficiency see Ref. 11.

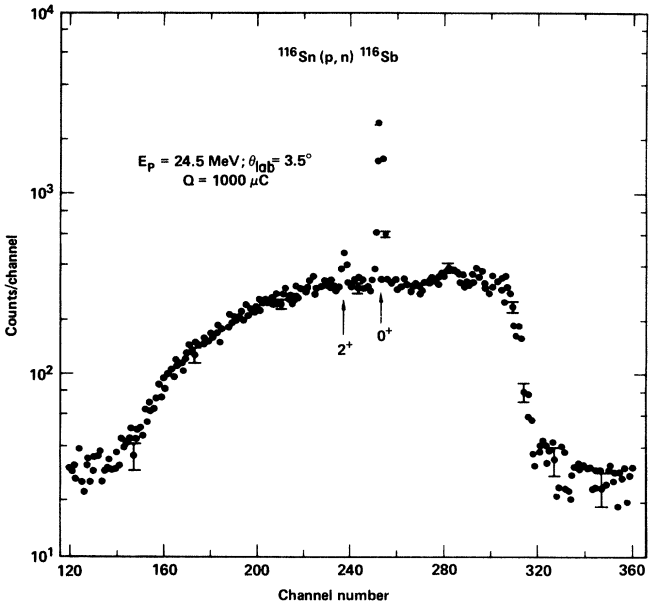

FIG. 1. Time-of-flight spectrum for ^{116}Sn(p,n)^{116}Sb at $\theta_{lab}=3.5°$ and 24.5 MeV bombarding energy. Increasing time of flight is towards the left. Time calibration of the system is 1.015 ns/channel. Clearly visible above the continuum are neutron groups populating the ground and 2^+ excited-analog states in ^{116}Sb.

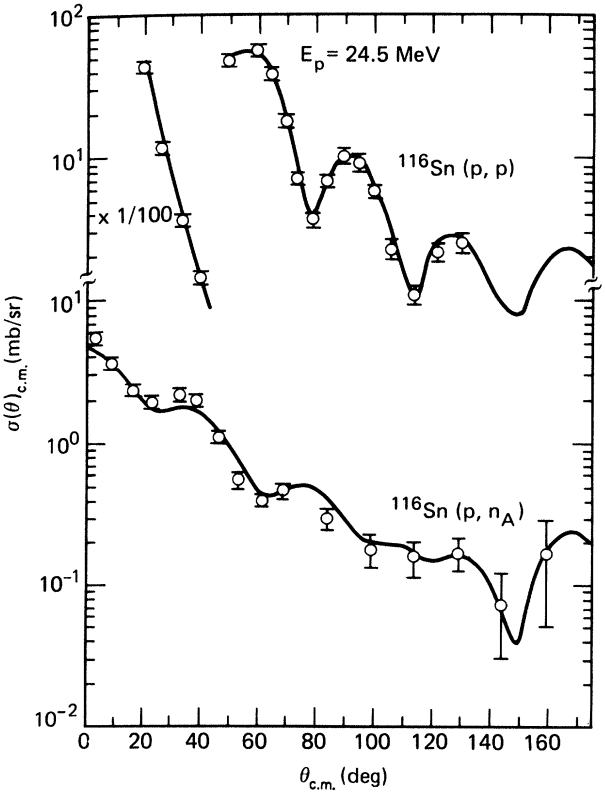

FIG. 2. Measured differential cross sections (bottom) for populating the ground state analog in ^{116}Sn(p,n) at 24.5 MeV, and (p,p) differential cross sections (top) generated using optical model parameters from Beer *et al.* Solid lines are simultaneous best fits generated using the search routine on the Lane coupled equations code.

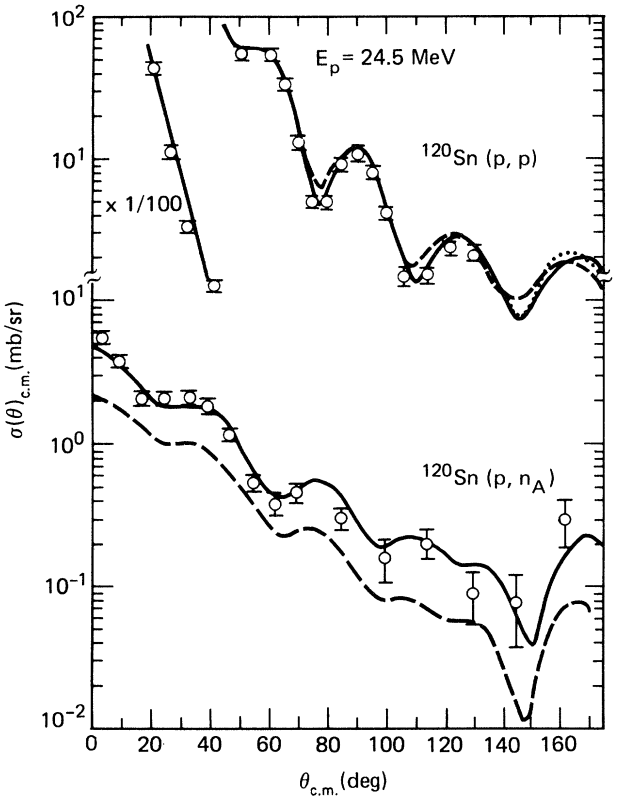

FIG. 3. Same as Fig. 2 except for ^{120}Sn. The dotted curve is the differential (p,p) cross sections calculated with the one-channel optical model code using coupled equations parameters. The dashed curves are the coupled equations predictions assuming no Coulomb correction on the imaginary potential starting from the Lane consistent neutron potential [Eq. (A3b)].

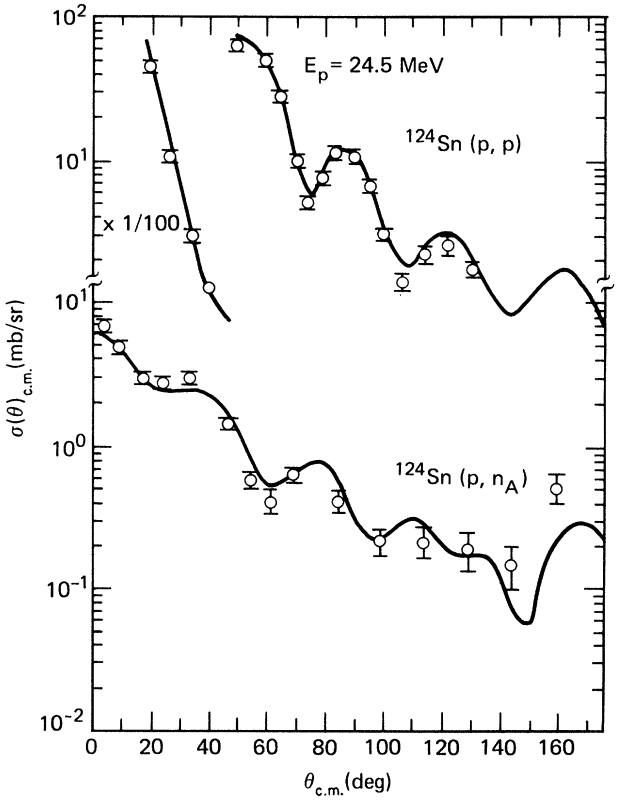

FIG. 4. Same as Fig. 2 except for ^{124}Sn.

EXPERIMENTAL RESULTS

Figure 1 shows a raw time-of-flight spectrum at $\theta_{lab}=3.5°$ for ^{116}Sn(p,n)^{116}Sb at a proton bombarding energy of 24.5 MeV. Clearly visible above the continuum are the neutron groups leading to the 0^+ ground and 2^+ excited-analog states in ^{116}Sb. The counts in the 0^+ group were extracted using a computer code which fitted a Gaussian to the peak. In all cases, a linear background was assumed. The extracted counts were converted to differential cross sections which are displayed for ^{116,120,124}Sn in the bottom half of Figs. 2—4, respectively. The errors on the differential cross sections are compounded from the counting statistics and the goodness of fit to the peaks. The plotted errors are the above errors or $\pm 7\%$, whichever is larger, the latter figure representing the absolute uncertainty in the detector efficiency. Our differential cross sections at 21.5 (Ref. 13) and 24.5 MeV for ^{116,124}Sn are consistent with the Colorado (p,n) measurements[14] at 22.8 MeV. A comparison of our differential cross sections for ^{120}Sn(p,n) at 24.5 MeV shows reasonable agreement with the 25 MeV measurements of Ref. 7.

LANE COUPLED EQUATIONS CALCULATIONS OF (p,p) AND (p,n) SCATTERING

The Lane coupled equations code[15] (LOKI 74), which provides an exact solution of the Lane coupled equations,

TABLE I. Isoscalar and isovector strengths in MeV.[a]

	^{116}Sn		^{118}Sn		^{120}Sn		^{122}Sn		^{124}Sn	
	Initial	Final	Initial	Final	Initial	Final	Initial	Final	Initial	Final
V_0	50.6	49.9	50.6	49.8	50.6	50.1	50.6	49.8	50.6	49.9
W_0	8.68	9.22	8.68	9.15	8.68	9.44	8.68	9.38	8.68	9.54
V_1	82.4	71.8	82.4	67.6	82.4	69.0	82.4	75.5	82.4	71.2
W_1	51.2	69.4	51.2	68.3	51.2	63.0	51.2	59.0	51.2	71.4
$\sqrt{V_1^2+KW_1^2}$[b]		89.2		85.3		84.0		87.9		89.6
χ^2(p,p)	1.08	0.77	3.23	1.00	2.47	1.22	2.81	1.50	1.99	1.80
χ^2(p,n)	3.34	2.43	9.6	1.65	14.3	1.92	8.55	2.13	4.53	3.26

[a] $U_0=V_0+iW_0$ and $U_1=V_1+iW_1$, with V_0 and V_1 having a Woods-Saxon volume and W_0 and W_1 having a derivative Woods-Saxon surface form factor.

[b] $K=k_2/k_1=0.58$, where $\sigma_T(\text{p,n})=k_2W_1^2$ and $\sigma_T(\text{p,n})=k_1V_1^2$, σ_T(p,n) obtained from LOKI 74 for ^{120}Sn.

was employed to calculate simultaneously (p,p) elastic and (p,n) quasielastic scattering. The geometrical and spin-orbit parameters were assumed to be identical for protons and neutrons and were taken from set A of the global Ohio University neutron potentials.[16] The Coulomb displacement energy was calculated from the expression $1.444\overline{Z}/A^{1/3}-1.13$ MeV (Ref. 17), where $\overline{Z}$ is the Z of the target plus $\frac{1}{2}$. The initial isoscalar and isovector strengths (see Table I) were obtained by comparing global set A at $E_n=11$ MeV with the U_{nn} parametrization of Eq. (2) and identifying the corresponding isoscalar and isovector real and imaginary components. A four-parameter search was then instituted on the volume-real and surface-imaginary isoscalar and isovector strengths to best fit the (p,p) and (p,n) data. In the search routine the isoscalar and isovector strengths were identical for protons and neutrons [see Eq. (2)], and the total neutron and proton potentials were automatically changed to reflect changes in the isoscalar and isovector strengths. Because tabular data were lacking, the (p,p) cross sections were generated from the one-channel optical model code LOKI 3D using optical parameters derived by Beer *et al.*, from their fits to the (p,p) data at 24.5 MeV. For each isotope, eighteen data points (see the top halves of Figs. 2—4) between 20° and 130° were chosen so as to characterize accurately the minima and maxima of the proton elastic scattering angular distributions. To ensure that the LOKI 74 search routine gave roughly equal weights to fitting the (p,p) and (p,n) data, the errors on the (p,p) elastic differential cross sections were made comparable to those of the (p,n) quasielastic data. These assigned errors varied from ±7% at the forward angles to ±15% at the back angles (see the top halves of Figs. 2—4). Fortuitously, these assigned errors are not unreasonable since Beer *et al.* quote an absolute cross section normalization uncertainty of ±15%.

Simultaneous best fits to the (p,p) and (p,n) data are shown as solid lines in Figs. 2—4 for ^{116,120,124}Sn. Similar quality fits were also obtained for ^{118,122}Sn. Within the quoted errors on the (p,p) and (p,n) cross sections, the search routine has provided acceptable fits to (p,p) and (p,n) data.

The best-fit isoscalar and isovector volume-real strengths (V_0, V_1) and surface-imaginary strengths (W_0, W_1) are listed in Table I along with the initial and final χ^2 values for the (p,p) and (p,n) channels. The observation (see Table I) that the (p,p) and (p,n) data are explicable in terms of a relatively constant "total" isovector strength $(\sqrt{V_1^2+kW_1^2})$ indicates that coupling to excited states[18] is fairly uniform over the isotopic sequence, and need not be included explicitly in the present analysis. The k factor obtained using LOKI 74 corrects for the fact that V_1 and W_1 are not equally effective in generating cross sections to the analog state. As required, the isoscalar strengths are also fairly constant. The small variation of the isoscalar and total isovector strengths could be due to the neglect of the coupling to the 2^+ and 3^- states.

(n,n) ELASTIC SCATTERING PREDICTIONS

Using U_{nn} of Eq. (2) to generate neutron parameters from the best-fit isoscalar and isovector strengths for each isotope, (n,n) elastic scattering at 11 MeV was calculated using the one-channel optical model code LOKI 3D. These predictions (solid lines) are compared with measurements[9] in Fig. 5. The agreement between our predictions and measurements is comparable to that obtained between the optimum fits (see Fig. 4, Ref. 9) and measurements. This would imply that our values of V and W are close to those of Ref. 9. An examination of Table II shows excellent agreement for ^{120}Sn and slightly poorer agreement for

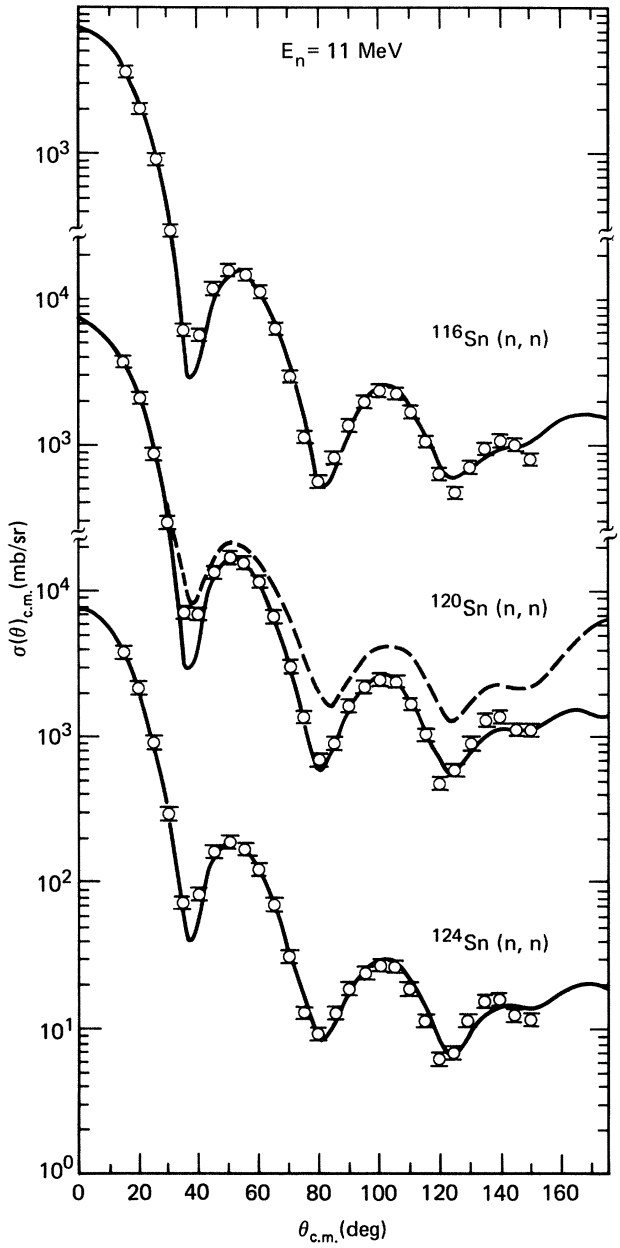

FIG. 5. ^{116,120,124}Sn(n,n) elastic scattering angular distributions at 11 MeV. Measurements are from Ref. 9. Solid lines are predictions employing the isovector and isoscalar strengths deduced from a simultaneous best fit to (p,p) and (p,n) data. Dashed curve for ^{120}Sn(n,n) is the prediction assuming no Coulomb correction for the imaginary potential while conserving the total imaginary proton strength obtained from the Lane coupled equations search code.

TABLE II. 11 MeV neutron parameters.

	^{116}Sn			^{118}Sn			^{120}Sn			^{122}Sn			^{124}Sn		
	a	b	c	a	b	c	a	b	c	a	b	c	a	b	c
V	47.51	47.72	47.72	47.22	47.41	47.25	47.23	47.12	47.13	46.40	46.85	47.00	46.45	46.56	46.73
			6.54			6.41			6.27			5.79			5.89
W	6.83	6.91	7.06[d]	6.55	6.72	6.92[d]	6.82	6.54	6.77[d]	6.72	6.38	6.25[d]	6.08	6.20	6.36[d]

[a]This work. Geometrical parameters taken from global set A (Ref. 16).
[b]Global set A.
[c]Reference 9. Optimum fits to (n,n) data.
[d]Reference 9. W corrected to geometrical parameters of a and b.

^{116,124}Sn. Table II also shows that our values of V and W are close to those obtained from global set A. Table I shows that a decreasing V_0 is compensated by a decreasing V_1, while an increasing W_0 is compensated by an increasing W_1, resulting in small changes in V and W from the global set A values.

The success of the Lane coupled equations in simultaneously fitting (p,p) and (p,n) at 24.5 MeV and subsequently (n,n) at 11 MeV is consistent with the assumption of a full Coulomb correction for both real and imaginary potentials for 24.5 MeV protons on the tin isotopes. In the Appendix, the neutron imaginary potential is derived on the assumption of no Coulomb correction while conserving the total proton imaginary potential obtained from the search routine. The prediction using this smaller imaginary potential is shown in Fig. 5 for ^{120}Sn(n,n) as a dashed line. Thus, independent of the information derived from the (p,n) channel, calculations of (n,n) scattering at 11 MeV do not agree with measurements if no Coulomb correction is assumed in the parametrization of the imaginary proton potential at 24.5 MeV.

In the Appendix, the proton imaginary potential is calculated assuming no Coulomb correction starting with the imaginary neutron potential of Eq. (A2b). The new imaginary proton potential is increased relative to the correct value given by the Lane coupled equations search routine. The new isoscalar imaginary strength $\tilde{W}_0''$ and isovector imaginary strength $\tilde{W}_1''$ (see the Appendix) are then inserted into LOKI 74 and (p,p) and (p,n) scattering calculated for ^{120}Sn. The results are shown as dashed curves in Fig. 3. Although the fit to the proton data is slightly poorer, the drastically lower (p,n) cross sections resulting from the lower imaginary isovector strength show the assumption of no Coulomb correction to be untenable.

As an additional check, the $\tilde{W}_0''$ and $\tilde{W}_1''$ values were regarded as different initial inputs into the search routine. After searching, the final best-fit isoscalar and isovector real and imaginary strengths were identical to those listed in Table I. Figure 3 also shows (dotted curve) ^{120}Sn(p,p) calculated with the one-channel optical model code LOKI 3D using values of parameters obtained from the LOKI 74 coupled equations search routine. With the exception of differences at $\theta > 150°$, the good agreement with the coupled equations result confirms that the coupling term is indeed small compared to the elastic scattering terms.

CONCLUSIONS

A straightforward application of the Lane coupled equations to fitting 24.5 MeV (p,p) and (p,n) data on the tin isotopes has yielded isoscalar and isovector potential strengths which produce very good fits to (n,n) data at 11 MeV. As discussed in the Introduction and Appendix, the applicability of the Lane coupled equations is consistent with the full Coulomb potential energy correction on the imaginary potential for the tin isotopes at 24.5 MeV bombarding energy. Furthermore, it was shown that the neutron and proton imaginary potentials, deduced from the corresponding best-fit proton and neutron potentials, respectively, assuming no Coulomb correction, yield

predictions which disagree with measurements. In addition, independent of (p,n) data, (p,p) scattering at 24.5 MeV and (n,n) scattering at 11 MeV are themselves consistent with a single Lane model optical potential only if the full Coulomb correction is applied to the imaginary proton potential.

Recent analyses of experiments on ^{40}Ca (Refs. 4 and 19) and ^{28}Si (Ref. 20) and theoretical calculations on ^{40}Ca (Refs. 21 and 22) and ^{208}Pb (Ref. 23) would suggest that the imaginary Coulomb correction is dependent on both energy and nuclear structure effects, and is approximately one-half the full Coulomb correction for ^{40}Ca and ^{208}Pb at 20–30 MeV bombarding energy. Using a microscopic folding model, Dietrich *et al.*[24] have found that good fits to ^{208}Pb(n,n) and ^{208}Pb(p,p) can be achieved only if the full Coulomb correction is invoked in evaluating the local momentum in the exchange calculation and no Coulomb correction is used in evaluating the energy dependent t matrix. It is thus surprising that the tin isotopes require the full Coulomb correction for the imaginary potential. The good agreement observed using the Lane coupled equations could well be due to energy dependent nuclear structure effects resulting in an effective full Coulomb correction for the tin isotopes at 24.5 MeV proton energy. Thus, it would be interesting to calculate the energy dependence of the imaginary Coulomb correction for the tin isotopes. In addition, the energy and mass regimes in which the full Coulomb correction on the imaginary potential is applicable can be investigated by applying the coupled equations to the tin isotopes at higher bombarding energies and to other nuclei (^{54}Fe, ^{56}Fe, ^{66}Zn, ^{208}Pb, etc.) provided appropriate (p,p), (p,n), and (n,n) experimental data exist.

ACKNOWLEDGMENTS

We are indebted to V. A. Madsen, C. H. Poppe, and V. R. Brown for helpful discussions. This work was supported at Lawrence Livermore National Laboratory under the auspices of the U.S. Department of Energy under Contract No. W-7405-ENG-48.

APPENDIX

In Eq. (2), U_0 and U_1 are in general complex and given by

$$U_0 = V_0 + iW_0 \ , \qquad U_1 = V_1 + iW_1 \ . \tag{A1}$$

The treatment of W_0 and W_1 with respect to energy dependence and Coulomb correction is similar to that for V_0 and V_1. Hence, in the following, only W_0 and W_1 will be considered. If W_0 and W_1 are linearly dependent on energy and if the proton imaginary potential is parametrized with the full Coulomb correction, the proton and neutron imaginary potentials are the following:

$$W_p = W_0(0) + \alpha E_p + \frac{(N-Z)}{4A}[W_1(0) - \beta E_p] - \frac{1.38Z}{A^{1/3}}\left[\alpha - \frac{\beta(N-Z)}{4A}\right] , \tag{A2a}$$

$$W_n = W_0(0) + \alpha E_n - \frac{(N-Z)}{4A}[W_1(0) - \beta E_n] \ . \tag{A2b}$$

If

$$E_p = E_n + \frac{1.38Z}{A^{1/3}} \text{ (full Coulomb correction)} \cong E_n + \text{CDE} \ ,$$

as is the case in the quasielastic (p,n) reaction, then

$$W_p = W_0(0) + \alpha E_n + \frac{(N-Z)}{4A}[W_1(0) - \beta E_n] = \tilde{W}_0 + \frac{(N-Z)}{4A}\tilde{W}_1 \ , \tag{A3a}$$

$$W_n = W_0(0) + \alpha E_n - \frac{(N-Z)}{4A}[W_1(0) - \beta E_n] = \tilde{W}_0 - \frac{(N-Z)}{4A}\tilde{W}_1 \ . \tag{A3b}$$

Hence, at bombarding energies differing by the CDE the effective isoscalar ($\tilde{W}_0$) and isovector ($\tilde{W}_1$) strengths are identical for protons and neutrons as specified by the Lane coupled equations.

A proton imaginary potential determined solely from fitting proton data and parametrized without explicit Coulomb correction terms is given by

$$W'_p = W'_0(0) + \alpha E_p + \frac{(N-Z)}{4A}[W'_1(0) - \beta E_p] \ . \tag{A4}$$

Comparison of Eq. (A4) with (A2a) shows that

$$W'_0(0) = W_0(0) - \left[\frac{1.38Z}{A^{1/3}}\right]\alpha \ , \qquad W'_1(0) = W_1(0) + \left[\frac{1.38Z}{A^{1/3}}\right]\beta \ . \tag{A5}$$

If $W'_0(0)$ and $W'_1(0)$ are then incorrectly interpreted as the zero energy isoscalar and isovector strengths, the resulting neutron potential is

$$W'_n = W'_0(0) + \alpha E_n - \frac{(N-Z)}{4A}[W'_1(0) - \beta E_n] \ , \tag{A6}$$

$$W'_n = W_n(\text{Lane}) - \left[\frac{1.38Z}{A^{1/3}}\right]\alpha - \left[\frac{N-Z}{4A}\right]\left[\frac{1.38Z}{A^{1/3}}\right]\beta \ .$$

Therefore in the Sn(p,n) reaction at $E_p = 24.5$ MeV, where a full Coulomb correction applies, the new imaginary neutron potential is reduced relative to the correct Lane coupled equations value [Eq. (A3b)].

Starting with the Lane consistent imaginary neutron potential of the form Eq. (A3b), the imaginary proton potential ignoring the Coulomb correction in the imaginary part is

$$W''_p = W_0(0) + \alpha E_p + \left[\frac{N-Z}{4A}\right][W_1(0) - \beta E_p] \ .$$

Substituting

$\left[E_n+\frac{1.38Z}{A^{1/3}}\right]$ for E_p yields

$$W_p''=\tilde{W}_0+\left[\frac{N-Z}{4A}\right]\tilde{W}_1+\frac{1.38Z}{A^{1/3}}\left[\alpha-\beta\left[\frac{N-Z}{4A}\right]\right] \quad \text{(A7)}$$

or

$$W_p''=W_p(\text{Lane})+\frac{1.38Z}{A^{1/3}}\left[\alpha-\beta\left[\frac{N-Z}{4A}\right]\right].$$

Since $\alpha\cong\beta$ and $[(N-Z)/4A]\ll 1$, the imaginary proton potential without Coulomb correction (W_p'') is increased from the correct Lane coupled equations value [Eq. (A3a)]. The proton imaginary potential, W_p'', can be expressed in terms of isoscalar and isovector components as follows:

$$W_p''=\tilde{W}_0''+\left[\frac{N-Z}{4A}\right]\tilde{W}_1'', \quad \text{(A8)}$$

where

$$\tilde{W}_0''=\tilde{W}_0+\left[\frac{1.38Z}{A^{1/3}}\right]\alpha=\tilde{W}_0(\text{Lane})+\left[\frac{1.38Z}{A^{1/3}}\right]\alpha, \quad \text{(A9a)}$$

and

$$\tilde{W}_1''=\tilde{W}_1-\left[\frac{1.38Z}{A^{1/3}}\right]\beta=\tilde{W}_1(\text{Lane})-\left[\frac{1.38Z}{A^{1/3}}\right]\beta. \quad \text{(A9b)}$$

In Eqs. (A9a) and (A9b), the isoscalar strength is increased while the isovector strength is decreased relative to the correct Lane coupled equations values. In all calculations, $\beta=0.31$ from Ref. 7 and α was deduced to be 0.174 from Ref. 4 for $E_p<25$ MeV.

*Present address: Physics Department, Ohio University, Athens, OH 45701.

[1]A. M. Lane, Nucl. Phys. 35, 676 (1962).
[2]G. R. Satchler, in *Isospin in Nuclear Physics*, edited by D. H. Wilkinson (North-Holland, Amsterdam, 1969), p. 411.
[3]F. D. Becchetti, Jr., and G. W. Greenlees, Phys. Rev. 182, 1190 (1969).
[4]J. Rapaport, Phys. Lett. 92B, 233 (1980).
[5]J. D. Carlson, C. D. Zafiratos, and D. A. Lind, Nucl. Phys. A249, 29 (1975).
[6]S. D. Schery, D. A. Lind, H. W. Fielding, and C. D. Zafiratos, Nucl. Phys. A234, 109 (1974).
[7]D. M. Patterson, R. R. Doering, and Aaron Galonsky, Nucl. Phys. A263, 261 (1976).
[8]O. Beer, A. El Behay, P. Lopato, Y. Terrien, G. Vallois, and K. K. Seth, Nucl. Phys. A147, 326 (1970).
[9]J. Rapaport, M. Mirzaa, H. Hadizadeh, D. E. Bainum, and R. W. Finlay, Nucl. Phys. A341, 56 (1980).
[10]J. C. Davis, J. D. Anderson, E. K. Freytag, and D. R. Rawles, IEEE Trans. Nucl. Sci. 20, 213 (1973).
[11]C. Wong, S. M. Grimes, C. H. Poppe, V. R. Brown, and V. A. Madsen, Phys. Rev. C 26, 889 (1982).
[12]R. C. Haight and D. R. Dalgas, Nucl. Instrum. Methods 165, 55 (1979).
[13]C. Wong *et al.* (unpublished).
[14]S. D. Schery, D. A. Lind, and Howard Wieman, Phys. Rev. C 14, 1800 (1976).
[15]E. H. Schwarcz, Phys. Rev. 149, 752 (1966).
[16]J. Rapaport, V. Kulkarni, and R. W. Finlay, Nucl. Phys. A330, 15 (1979).
[17]J. D. Anderson, C. Wong, and J. W. McClure, Phys. Rev. 138, B615 (1965).
[18]For a complete bibliography see Ref. 11.
[19]W. Tornow, Nucl. Phys. A 385, 373 (1982).
[20]R. De Leo and W. A. Sterrenburg, Kernfysisch Versneller Institut Annual Report, 1980, p. 8.
[21]F. Osterfeld and V. A. Madsen, Phys. Rev. C 24, 2468 (1981).
[22]L. G. Arnold and B. C. Clark, Phys. Lett. 84B, 46 (1979).
[23]J. P. Jeukenne, A. Lejeune, and C. Mahaux, Phys. Rev. C 15, 10 (1977); 16, 80 (1977).
[24]F. S. Dietrich, R. W. Finlay, S. Mellema, G. Randers-Pehrson, and F. Petrovich, Phys. Rev. Lett. 51, 1629 (1983).